1
Genetic Watermarking for Copyright Protection

Hsiang-Cheh Huang[1], Chi-Ming Chu[2], and Jeng-Shyang Pan[2]

[1] National University of Kaohsiung,
Kaohsiung 811, Taiwan, R.O.C.
huang.hc@gmail.com
http://hchuang.ee.nuk.edu.tw/
[2] National Kaohsiung University of Applied Sciences,
Kaohsiung 807, Taiwan, R.O.C.
jspan@cc.kuas.edu.tw
http://bit.kuas.edu.tw/~jspan

Summary. Applications for robust watermarking is one of the major branches in digital rights management (DRM) systems. Based on existing experiences to assess how good one robust watermarking is, it is generally agreed that three parameters or requirements, including the quality of watermarked contents, the survivability of extracted watermark after deliberate or unintentional attacks, and the number of bits embedded, need to be considered. However, performances relating to these three parameters conflict with each other, and the trade off must be searched for. In this chapter, we take these requirements into consideration, and we can find the optimized combination among the three parameters. With the aid of genetic algorithm, we design an applicable system that would obtain the good quality, acceptable survivability, and reasonable capacity after watermarking. Simulation results present the effectiveness in practical implementation and possible application of the proposed algorithm.

1.1 Introduction

Multimedia contents are easily spread over the Internet. Due to the ease of delivery and modification of digital files, the copyrights might be infringed upon. To deal with this problem, digital rights management (DRM) systems can prevent users from using such contents illegally [3]. In DRM systems, *encryption* and *robust watermarking* are two major schemes for applications [6, 7, 10]. By using encryption to protect data, the encrypted digital contents look like random and noisy patterns, which will cause the eavesdroppers to suspect the existence of hidden secrets. Furthermore, if one bit is received erroneously during transmission, part or whole of received data would not be decrypted, leading to the uselessness of such contents. Under

J.-S. Pan et al. (Eds.): Information Hiding and Applications, SCI 227, pp. 1–19.
springerlink.com

the umbrella of watermarking researches, the main goal is to cope with the deliberately or unintentionally applied modifications, called attacks, and such a kind of watermarking schemes is regarded as robust watermarking.

On the other hand, watermarking can be classified into two major categories; one is fragile watermarking (also named data hiding or steganography), and the other is robust watermarking. For fragile watermarking, the watermarked content looks identical to its original counterpart, and it cannot withstand the slightest modification intentionally or unintentionally, since it would lead to the result that the embedded watermark gets vanished. From this viewpoint, fragile watermarking and encryption are similar since they are vulnerable to modifications. For robust watermarking, the watermarked contents and their original counterparts look similar, or even identical from subjective point of view. The major advantage for robust watermarking is that the watermark embedded can survive even when the watermarked content gets modified. Thus, we focus on robust watermarking and propose an applicable solution with optimization techniques in DRM implementation.

In this chapter, we use the digital images to represent the multimedia contents. It is generally agreed that for one robust watermarking algorithm, the watermarked image quality (or *imperceptibility*), the survivability, represented by the correct rate of extracted watermark (or *robustness*), and the number of bits embedded (or *capacity*), are the three most important factors to assess how good the algorithm and implementation are. However, some trade off must be searched for because the three factors conflict with each other. Here we employ genetic algorithm (GA) [1] to find an optimized solution numerically that can reach better imperceptibility, more robustness, and reasonable capacity. The scheme can be directly applicable to DRM systems.

This chapter is organized as follows. In Section 1.2 we point out the need for optimization in a watermarking system. In Section 1.3 we describe proposed algorithm by modifying and extending previous works. Two detailed case studies are presented in Section 1.4, and simulation results are demonstrated in Section 1.5. Finally, we make conclusions in Section 1.6.

1.2 Watermarking Requirements

As we stated in Section 1.1, the three major requirements for robust watermarking are imperceptibility, robustness, and capacity. Their interrelationships can be discussed as follows. And we can see why they conflict with each other, and the tradeoff among the three should be reached with the aid of optimization techniques.

1.2.1 Watermark Imperceptibility

Watermark imperceptibility refers to whether the viewer can perceive the existence of embedded watermark or not from subjective point of view [2, 13].

It also means the quality of the watermarked image, measured by the distortion induced between the watermarked and original images due to watermark embedding, and it is represented by numerical values such as the Peak Signal-to-Noise Ratio (PSNR) objectively. The PSNR has the definition in Eq. (1.1). Let the original image and the watermarked one be $\boldsymbol{X}$ and $\boldsymbol{X}'$, respectively, with image size of $M \times N$. The PSNR is

$$\mathrm{PSNR} = 10 \times \log_{10} \left(\frac{255^2}{\frac{1}{M \times N} \sum_{i=1}^{M} \sum_{j=1}^{N} \left(X(i,j) - X'(i,j) \right)^2} \right). \quad (1.1)$$

Larger PSNR values imply less distortions induced, hence the better outcomes can be reached.

For getting the better imperceptibility, less modification to the original content is desired. Hence, we can lead to the derivations as follows.

- Embedding more bits induce more distortion into the original image. Thus, embedding fewer bits, namely, decreasing the capacity, meets the goal.
- If we set the capacity a constant value, embedding bits into least significant bit or higher frequency coefficient would alter the image as less as possible. However, this would degrade the robustness since the watermarked image may experiencing filtering and the hidden watermark may get vanished.

1.2.2 Watermark Robustness

Watermark robustness means the capability that the watermarked media can withstand deliberate or unintentional media processing, called attacks, including filtering, resizing, or rotation [6, 7]. There are also benchmarks to perform attacks [8]. From subjective viewpoint, the extracted watermark needs to be as similar as the embedded one. And speaking objectively, the correlation between the two needs to be measured. People often use the bit correct rate (BCR), with the definition in Eq. (1.2), to assess the robustness of the watermarking algorithm. The normalized cross-correlation (NC) between the embedded watermark and the extracted one may also be considered to assess the survivability for the extracted watermark. Let the embedded and extracted watermarks be $\boldsymbol{W}$ and $\boldsymbol{W}'$, respectively, with size of $M_W \times N_W$. With its ease of calculation, we choose the BCR values to measure the robustness of extracted watermarks. The BCR is

$$\mathrm{BCR} = 1 - \frac{1}{M_W \times N_W} \sum_{i=1}^{M_W} \sum_{j=1}^{N_W} \left[W(i,j) \oplus W'(i,j) \right], \quad (1.2)$$

where $\oplus$ denotes the exclusive-or (XOR) operation. The larger the BCR value, the better the result. To make the algorithm robust, the watermark needs to be hidden into more important parts, such as the most significant bits or the low frequency components, in order to resist common attacks.

- In addition to obtaining the larger BCR value, extracted watermark needs to be recognizable. Based on this standpoint, the capacity should be more than some pre-determined threshold value.
- Embedding bits into lower frequency coefficient would increase the robustness. However, this would sacrifice the imperceptibility.

1.2.3 Watermark Capacity

Watermark capacity attributes to the number of bits embedded into the original media, that is, the size of watermark. We can see that from the results in [11], embedding more bits into the contents would directly cause the degradation of the quality of watermarked image. On the contrary, embedding too few bits may lead to the result that the extracted watermark may hardly be comprehensible even though the watermarked image quality can be guaranteed. Thus, the watermark capacity needs to be carefully chosen to be meaningful.

- Even though increasing the capacity is desired, the appropriate number of capacity should lie above some threshold in order to make the extracted watermark recognizable. On the other hand, embedding too many bits may sacrifice the imperceptibility. If the increase in capacity is feasible under the condition that acceptable quality in watermarked image is obtained, using error control codes (ECC) [5] for encoding the watermark is a able way to meet the requirement.
- Once the capacity is determined, embedding into higher frequency coefficients meets the goal for imperceptibility. On the contrary, embedding into lower frequency coefficients meets the goal for robustness. Hence, some trade off must be searched for, and this is the major contribution of the paper in [12].

1.2.4 Optimization for Requirements

Since there are conflicts among the three requirements described in Secs. 1.2.1 to 1.2.3, we employ the optimization technique for finding the better outcome. First, the fitness function should be designed. Next, parameters relating to the optimization technique should be carefully chosen.

From the above discussions, we lead to the results that better imperceptibility, more robustness, and the reasonable number of capacity are all required for designing the algorithm. For measuring imperceptibility, we use PSNR of watermarked image to serve as an objective measure. In evaluating robustness, after applying some deliberate attacks [2], we calculate the BCR. For measuring capacity, we count the average number of bits, C, embedded into one 8×8 block, since we are going to embed the watermark with discrete cosine transform (DCT). The fitness function for training at iteration i can be defined:

$$f_i = \mathrm{PSNR}_i + \lambda_1 \cdot \frac{1}{n} \sum_{k=1}^{n} \mathrm{BCR}_{k,i} + \lambda_2 \cdot C_i. \tag{1.3}$$

The first term, PSNR_i, denotes the imperceptibility. In the second term, because we expect to cope with n different attacks, we calculate the robustness after certain attacks, $\mathrm{BCR}_{k,i}$, respectively, and the average of these BCR values is served as the robustness measure. In the third term, C_i implies the capacity. Because PSNR values are usually more than 30 dB, the BCR values lie between 0 and 1, and the capacity can be set to 1 to 4 bits per block after considering practical situations, and the average capacity must lie between 1 and 4 bit/block, we find that values corresponding to the three components lie into various ranges because of their inherent characteristics. Thus, we introduce two weighting factors, λ_1 and λ_2, into the fitness function. The main reason is to balance the effects and contributions from these three factors. And the goal of our optimization algorithm is to find the maximum value in Eq. (1.3).

Figure 1.1 is the conceptual illustration of robust watermarking with GA optimization. Original image $\boldsymbol{X}$ is the input. At the beginning, we set the number of iteration for training. In the training process, for every population in GA, the number of bits for embedding into every 8×8 block of the original image, one after another, is decided first, and the watermark capacity is regarded as one of the three parts in the fitness function. Next, the watermark is embedded into the original images, namely, the populations in GA, and the PSNR values of watermarked images are obtained. Finally, we apply n different attacks, for instance, JPEG compression for every population, and we try to extract the embedded watermarks from every attacked image. The BCR values between the embedded and extracted watermarks under different attacks are obtained. After calculating the fitness function, we proceed with this process in the next iteration until meeting the terminating condition. Finally, the optimized, watermarked image, $\boldsymbol{Y}$, and associated secret key, key_1, are delivered to the reception side.

1.3 Proposed Algorithm

We employ genetic algorithm (GA) for optimizing the three requirements above. GA is constituted of three major steps: *selection*, *crossover*, and *mutation* [1]. Based on the fitness function in Eq. (1.3) and the dashed box on the left side of the flow graph in Figure 1.1, we propose an integration of our watermarking scheme with GA procedures.

1.3.1 Preprocessing in GA

GA is a process to emulate the natural selection. We need to have populations for training in GA to perform the three steps. The number of populations is generally chosen to be an even number to ease the operation of the crossover step.

Every population is composed of chromosomes. The chromosome is a binary string, and the binary representation denotes the positions for watermark embedding in one block. It has variable length, which depends on the

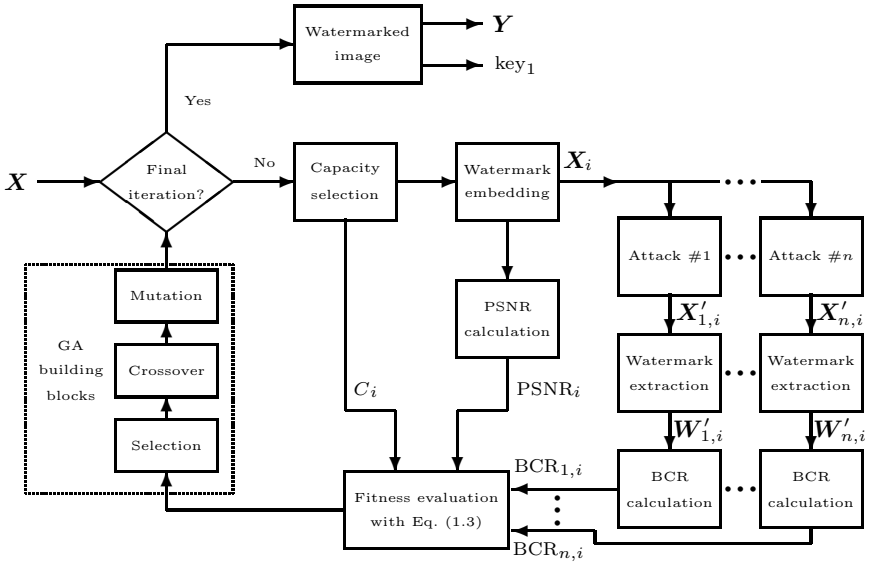

Fig. 1.1. Building blocks of watermarking with GA-based optimization schemes

watermark capacity decided. By concatenating the binary string of every block in the image, we obtain one population in GA. Because we perform 8×8 DCT for watermark embedding [12], we have 64 DCT coefficients, ranging between 0 and 63, and these coefficients are represented with a 6-bit string, in one block. If the size of original image is $W \times H$, and let the maximal capacity be $C_{\max}$ bit/block, the length of the population is $\frac{W}{8} \times \frac{H}{8} \times 6 \times C_{\max}$ bits. For certain blocks that are embedded fewer bits than $C_{\max}$, considering the practicability in implementation, the remaining parts of the chromosome are replaced by consecutive bits of 0's. The size of original image is 512×512 and that of the binary watermark is 128×128 in this chapter. Hence, $C_{\max}$ is set to be $\frac{128 \times 128}{\left(\frac{512}{8} \times \frac{512}{8}\right)} = 4$ bit/block.

1.3.2 Deciding the Capacity in One Iteration

After considering practical implementations in GA in Sec. 1.3.1, $C_{\max} = 4$. And the capacity for every 8×8 block is variable, ranging between 1 to 4 bits per block. After calculation of 8×8 DCT, 64 DCT coefficients can be produced, and the range lies between 0 and 63, where 0 denotes the DC coefficient, i denotes the i^{th} AC coefficients, $1 \leq i \leq 63$ for watermark embedding.

For clearly explaining our implementation, we describe an instance as follows. If the capacity $C = 3$ for a certain block, and suppose that the 19^{th}, 28^{th} and 43^{th} coefficients are selected, then the chromosome in this block is represented by a 24-bit string `010011 011100 101011 000000`, where the 18 bits in the first three segments denote the position, and the final 6 bits

represent the remaining positions that are not selected, which are intentionally inserted to ease the implementation. At the first training iteration, all the AC coefficients are randomly selected for watermark embedding.

1.3.3 Embedding Watermark with DCT

We modify conventional schemes [12] for DCT-based watermarking to embed the binary watermark.

Step 1. Perform DCT on original image: 8×8 DCT is performed on the entire 512×512 image. For one block, it leads to one DC coefficient, presented by coefficient 0, and 63 AC coefficients, presented by coefficients 1 to 63.

Step 2. Determine the capacities and positions: The goal of our algorithm is to search for the proper positions for embedding based on decided capacity, leading to a trade off among the three requirements and suitable positions.

Step 3. Obtain the threshold for embedding: The average values of DC and other 63 AC coefficients among the $\frac{512}{8} \times \frac{512}{8}$, or 4096 blocks are served as the thresholds for watermark embedding.

Step 4. Embedding the watermark: The thresholds in Step 3 sre represented by a vector $\boldsymbol{a} = [a_0, a_1, \cdots, a_{63}]$, where $\boldsymbol{a}$ denotes the average value. The DC coefficient is prohibited for embedding. And we use the vector $\boldsymbol{r} = \left[\frac{a_0}{a_1}, \frac{a_0}{a_2}, \cdots, \frac{a_0}{a_{63}}\right]$ to serve as the reference for modifying the AC coefficients, where $\boldsymbol{r}$ denotes the ratio between DC and AC coefficients. Embedding of watermark meets one of the two situations below.

- If bit 0 is embedded, the AC coefficient in selected position is modified. If it is larger than the reference value in $\boldsymbol{r}$, it is decreased to be smaller than the corresponding element in $\boldsymbol{r}$ by a parameter δ. If not, the value is kept unchanged.
- If bit 1 is embedded, the coefficient is modified to be in contrary with the previous condition.

Step 5. Perform the inverse DCT on modified coefficients: Inverse DCT is calculated to obtain the watermarked image. The corresponding positions for watermark embedding are also recorded, and the PSNR of the watermarked image can be obtained.

1.3.4 Choosing Proper Attacks

For verifying robust watermarking, applying attacks to watermarked image is necessary. However, attacks need to be properly selected such that the attacked images still retain its meaningfulness and commercial value. For instance, image cropping attack is unsuitable since too much information would be discarded, and subjective image quality is degraded. Here, we choose three kinds of attacks [8], namely, JPEG compression with different quality

factors (QF), low-pass filtering (LPF), and median filtering (MF), to perform the attacks. Attacked images look similar to their original counterpart after applying these properly selected attacks. The BCR values after experiencing these attacks are calculated, and the average of these values are included into the fitness function.

1.3.5 Extracting the Watermark

Let the watermarked image $\boldsymbol{Y}$ in Figure 1.1, after applying attack, be denoted by $\boldsymbol{Z}$. We calculate the DCT of the attacked image $\boldsymbol{Z}$, and generate the new reference value $\boldsymbol{r}'$ by following Step 4 in Sec. 1.3.3. The extracted watermark bit is determined by one of the two situations below.

- If the selected coefficient divided by the average of DC value in $\boldsymbol{Z}$ is smaller than its corresponding coefficient in $\boldsymbol{r}'$, we decide the extracted watermark bit to be 0;
- If the selected coefficient divided by the average of DC value in $\boldsymbol{Z}$ is larger than its corresponding coefficient in $\boldsymbol{r}'$, we decide the extracted watermark bit to be 1.

1.3.6 Evaluating Fitness

We gather the average capacity C in Sec. 1.3.2, calculate the PSNR in Step 5 of Sec. 1.3.3, and obtain the average of BCR in Secs. 1.3.4 and 1.3.5, and then combine them altogether to calculate the fitness value with Eq. (1.3). Every population corresponds to one fitness value in the training iteration.

1.3.7 GA Procedures

The generated binary strings are ready for GA procedures. In this chapter, the number of populations is 10. The selection rate is 0.5, meaning that only the 5 populations with higher fitness values are kept for the next iteration, and the remaining 5 are produced by the crossover operation. The mutation rate is 0.1, meaning that 10% of all the bits are randomly selected and intentionally flipped. The main theme for GA is to search for the proper coefficient positions for watermark embedding, leading to the associated secret key, key_1. The secret key can be delivered with the scheme in [9]. Weighting factor λ_1 is set to be between 0 and 200, and its counterpart λ_2 is set to range between 0 and 50 in the GA training process. The parameter for altering the selected DCT coefficients in Step 4 in Sec. 1.3.3, δ, is fixed to 5. The major reason for choosing these values is to balance the effects from the three requirements, because we would like to have equal contribution from the three requirements to some extent. Based on this setting, fitness value from the three weighted requirements can lie among the following ranges:

- PSNR part: from 30 to 55, observed from simulation results;
- BCR part multiplied by weighting factors: from 0 to 200, because BCR $\in [0, 1]$ and $\lambda_1 \in [0, 200]$;
- capacity part multiplied by weighting factors: from 0 to 200, because $C \in [1, 4]$ and $\lambda_2 \in [0, 50]$.

Results with these different combinations of weighting factors are verified in Sec. 1.5.

1.3.8 The Stopping Condition

Once the number of training iterations in GA is reached, the optimization process is stopped. The population with the largest fitness value in the final iteration is the optimized watermarked image. Corresponding secret key with this image is also delivered to the receiver [9].

1.4 Case Studies in Optimized Embedding

1.4.1 Fixed Embedding Capacity

We choose the test image `bridge` with the picture size of 512×512, illustrated in Figure 1.2(a). The binary watermark with the size of 128×128 is prepared, shown in Figure 1.2(b). In Figure 1.2, the width and height between the two images are carefully chosen to be 4 : 1. And we will compare with the results shown in [12]. Because in [12], authors used normalized correlation (NC) to represent the watermark robustness, and we use BCR here, hence we show extracted watermarks for subjective evaluation in Figure 1.3. Both [12] and here we denote imperceptibility by using PSNR, we make comparisons in Table 1.1. Based on the settings by including JPEG quantization tables with watermarking in [12] for reference, we obtain reasonable results with the algorithm proposed in this chapter.

We choose the JPEG attack with quality factor QF = 80 to validate the proposed algorithm. The weighting factors, λ_1 and λ_2 in Eq. (1.3), are set to $\lambda_1 = 50$ and $\lambda_2 = 0$, respectively. The main reason for setting $\lambda_2 = 0$ is that we can manually adjust the capacity to see the performances between imperceptibility and robustness. First, we compare the extracted watermarks in Figure 1.3. Figure 1.3(a) shows the one with capacity of 4 bit/block. Figure 1.3(b)–(d) illustrate those with capacity of 3, 2, 1 bit/block, respectively, leading to the watermark size of 128×96, 128×64, and 128×32. Figure 1.3(a) can be clearly perceived, and the BCR value is high. We can also see that in Figure 1.3(b), the capacity is 3 bit/block, and only the upper three quarters can be recognized. The bottom quarter is intentionally set to bit 0 for comparison. Figure 1.3(c) and (d) also have similar phenomena. For embedding 3 or 4 bit/block, similar BCR values can be obtained. When decreasing the

(a) Original `bridge` image (b) Watermark

Fig. 1.2. (a) The original `bridge` image with size 512×512. (b) The binary watermark with size 128×128.

capacity to 2 or 1 bit/block, the BCR values grow. However, even though the BCR values are high enough, decreasing the capacity leads to be less meaningful in the extracted watermarks.

Table 1.1 makes comparison between our scheme and that in [12]. We can see that comparable results can be obtained. When we lower the embedded capacity, the PSNR values get higher. This is because less DCT coefficients get modified, and it proves our discussions in Sec. 1.2.

Table 1.1. Comparisons of capacity (in bit/block) and imperceptibility, represented by PSNR (in dB), between our algorithm and existing one

Scheme	Capacity	Imperceptibility
Existing ([12])	4 bit/block	34.79 dB
Proposed	4 bit/block	33.95 dB
	3 bit/block	35.24 dB
	2 bit/block	37.57 dB
	1 bit/block	40.50 dB

In Figure 1.4, we present the number of embedded positions that is associated with the results in Figure 1.2. Due to the JPEG compression attack that tends to discard the higher frequency coefficients, lower to middle frequency coefficients, namely, AC_2 and AC_{18}, are mostly embedded. Moreover, with the values indicated on the vertical axis, we can see that the total number of embedded bits decreases from Figure 1.4(a) to Figure 1.4(d).

From the data in Figure 1.3, Figure 1.4, and Table 1.1 above, we can find out that the three requirements have their own characteristics inherently, and they influence on another. By taking the watermark capacity into account, we have more flexibility in the design of algorithm.

1.4.2 Variable Embedding Capacity

Considering the fitness function in Eq. (1.3), we choose $\lambda_1 = 50$ and $\lambda_2 = 15$ for the detailed case study among the three requirements. The main reason for choosing such values is to balance the contributions from all the three requirements. Regarding to the attacking schemes, the JPEG compression with QF = 80 is chosen for verifying our algorithm in this case study. Moreover, attacking schemes with the 3×3 low-pass filtering (LPF), and the 3×3 median filtering (MF), are also examined, and results are depicted in Sec. 1.5. In GA, we choose 20 populations with selection rate of 0.5 and mutation rate of 0.1 for optimization.

After training for 100 iterations under the preliminary for better imperceptibility and better robustness under the JPEG attack, we obtain the optimized output with PSNR = 45.91 dB in Figure 1.5, and we can hardly

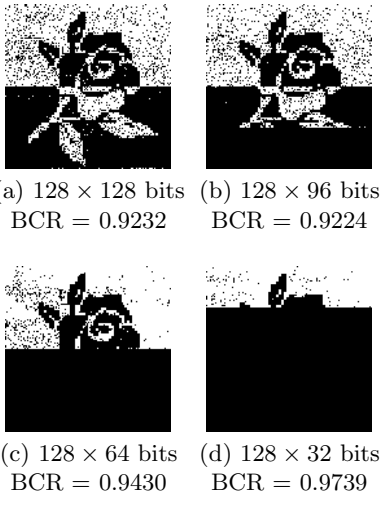

(a) 128×128 bits BCR = 0.9232 (b) 128×96 bits BCR = 0.9224

(c) 128×64 bits BCR = 0.9430 (d) 128×32 bits BCR = 0.9739

Fig. 1.3. (a)–(d) Extracted watermarks with capacities 4, 3, 2, and 1 bit/block, respectively

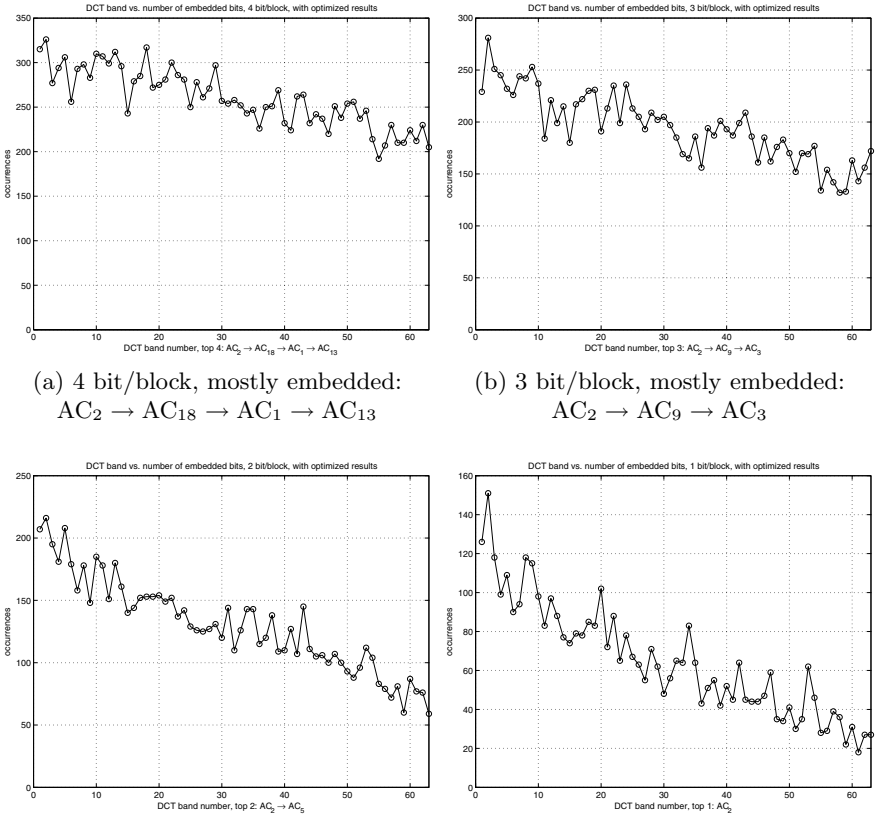

(a) 4 bit/block, mostly embedded: $AC_2 \rightarrow AC_{18} \rightarrow AC_1 \rightarrow AC_{13}$

(b) 3 bit/block, mostly embedded: $AC_2 \rightarrow AC_9 \rightarrow AC_3$

(c) 2 bit/block, mostly embedded: $AC_2 \rightarrow AC_5$

(d) 1 bit/block, mostly embedded: AC_2

Fig. 1.4. The histogram between embedding DCT coefficients and the number of bits embedded. (a)–(d) Embedding coefficients with capacity 4, 3, 2, and 1 bit/block, respectively.

differentiate the differences between the original image and the watermarked one subjectively. Regarding to the watermark robustness in addition to the JPEG attack, we also employ two other attacking schemes altogether on the watermarked image to see whether our attack can survive after other attacks or not. For making comparisons conveniently, we put the embedded watermark again in Figure 1.6(a). And we can see that BCR = 0.9603 for JPEG attack in Figure 1.6(b), BCR = 0.7128 for LPF attack in Figure 1.6(c), and BCR = 0.7469 for MF attack in Figure 1.6(d).

It is easily comprehended that in this case, we can obtain better imperceptibility and it can successfully resist the JPEG attack. However, it cannot survive under other attacks, such LPF and MF due to the fact that the BCR after JPEG attack is included into the fitness function in GA in Eq. (1.3),

Fig. 1.5. Watermarked output, PSNR = 45.91 dB

watermark
(a)

JPEG attack, BCR = 0.9603
(b)

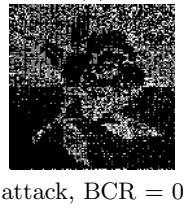

LPF attack, BCR = 0.7128
(c)

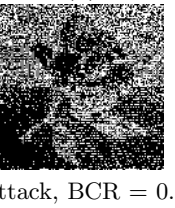

MF attack, BCR = 0.7469
(d)

Fig. 1.6. Comparisons of embedded watermark and extracted ones after different attacks. From subjective viewpoint, (c) and (d) do not survive well under LPF and MF attacks. (a) Embedded watermark containing $128 \times 128 = 16384$ bits. (b) Extracted from JPEG attack. (c) Extracted from LPF attack. (d) Extracted from MF attack.

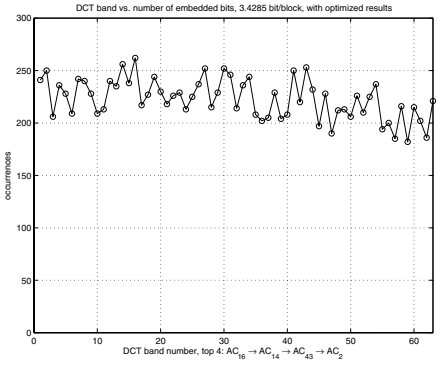

Fig. 1.7. The histogram between embedding DCT coefficients and the number of bits embedded. AC_{16} and AC_{14} are the top-two coefficients for embedding, and a total of 14043 bits, or 3.4285 bit/block, are embedded.

but others are not. With this observation, when coping with several different attacks, all the extracted BCR values need to be integrated into the fitness function. For clearly representing the effects under various capacities, in the extracted watermark, bit 0 and bit 1 are denoted by black and white pixels, respectively, while those in the remaining parts are intentionally denoted by grey pixels. This phenomena can be seen from Figure 1.6(b) to Figure 1.6(d). On the one hand, the watermark extracted from JPEG-attacked image, shown in Figure 1.6(b), can be clearly recognizable, and the BCR value is very high. On the other hand, the watermark extracted from LPF- and MF-attacked image, illustrated in Figures 1.6(c) and (d), respectively, can hardly be recognized, and also the BCR values are not high enough. This result is reasonable because we focus on the JPEG attack, and Figure 1.6(b) verifies this phenomenon.

Next, we check the histogram for embedding coefficients in Figure 1.7, and we find that a total of 14043 bits are embedded. For measuring imperceptibility, objective value is acceptable and most parts for watermarking are invisible. For evaluating robustness, the BCR value is high enough, while the extracted watermark is easily recognized under JPEG attack. For embedding positions, the 16^{th} and 14^{th} coefficients (or AC_{16} and AC_{14}, respectively) are embedded mostly, which follows the concept of embedding into 'middle frequency bands' proposed in literature [2, 12].

1.5 Simulation Results

1.5.1 Selection of Weighting Factors

Besides the case study depicted in Sec. 1.4, we provide more results with our experiments as follows. Table 1.2 demonstrates the performances among

imperceptibility, robustness, and capacity, and the two DCT coefficients that are mostly embedded, under a variety of weighting factors. These results are obtained after 100 training iterations in GA, with selection rate of 0.5 and mutation rate of 0.1. We perform lots of experiments based on the preliminary conditions that $\lambda_1 \in [0, 200]$ and $\lambda_2 \in [0, 50]$, and we present results with 15 of all the experiments in Table 1.2. These experiments can be classified into three categories:

1. fixing the robustness factor λ_1 to 50, and varying the capacity factor λ_2 from 10 to 30 with a stepsize of 5.
2. fixing the robustness factor λ_1 to 100, and varying the capacity factor λ_2 from 10 to 30 with a stepsize of 5.
3. fixing the robustness factor λ_1 to 150, and varying the capacity factor λ_2 from 10 to 30 with a stepsize of 5.

From the numerical values in Table 1.2, and the subjective evaluation from Figure 1.9, we observe that by increasing the weighting factor of capacity, we can see that the average capacity gets increased, while the BCR values gets somewhat reduced. PSNR values fluctuate a bit, but comparing to the original image, they remain objectively unnoticed in the watermarked parts. It is because of the embedding position selected after GA optimization. According to the data presented in Figure 1.8, the best embedding bands also lie in low to middle frequency bands.

Table 1.2. Comparisons of imperceptibility (in dB), robustness, and capacity (in bit/block) with different weighting factors

PSNR (dB)	BCR (JPG)	BCR (LPF)	BCR (MF)	Capacity (bit/block)	The two best bands	Factors λ_1	Factors λ_2
45.46	0.9161	0.7897	0.8484	3.3364	$AC_4 \rightarrow AC_2$	50	10
44.34	0.9013	0.7199	0.8103	3.7200	$AC_4 \rightarrow AC_2$	50	15
43.23	0.8838	0.6698	0.7695	3.9302	$AC_1 \rightarrow AC_{12}$	50	20
43.01	0.8820	0.6611	0.7599	3.9819	$AC_7 \rightarrow AC_4$	50	25
42.95	0.8824	0.6598	0.7588	3.9941	$AC_1 \rightarrow AC_2$	50	30
41.58	0.9349	0.8799	0.9011	2.8264	$AC_4 \rightarrow AC_1$	100	10
40.98	0.9402	0.8268	0.8959	3.1804	$AC_1 \rightarrow AC_4$	100	15
40.94	0.9308	0.7875	0.8681	3.5144	$AC_4 \rightarrow AC_1$	100	20
40.33	0.9118	0.7374	0.8375	3.7473	$AC_4 \rightarrow AC_1$	100	25
39.92	0.9058	0.7054	0.8167	3.8752	$AC_1 \rightarrow AC_4$	100	30
40.78	0.9421	0.8762	0.9181	2.7021	$AC_4 \rightarrow AC_2$	150	10
39.94	0.9530	0.8871	0.9215	2.8979	$AC_4 \rightarrow AC_2$	150	15
39.90	0.9534	0.8683	0.9131	3.1506	$AC_4 \rightarrow AC_1$	150	20
39.55	0.9420	0.8304	0.8994	3.3611	$AC_1 \rightarrow AC_4$	150	25
38.99	0.9332	0.7838	0.8702	3.5781	$AC_4 \rightarrow AC_1$	150	30

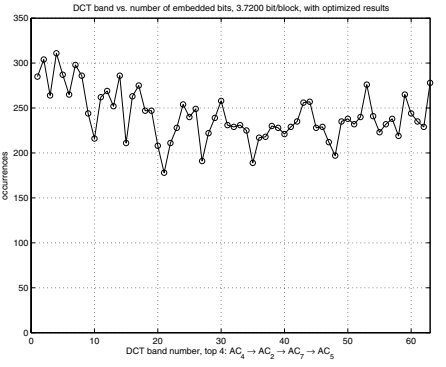

(a) $\lambda_1 = 50$ and $\lambda_2 = 15$

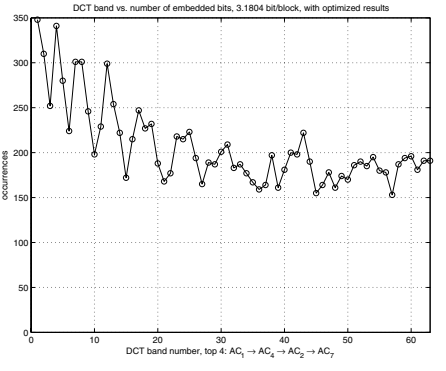

(b) $\lambda_1 = 100$ and $\lambda_2 = 15$

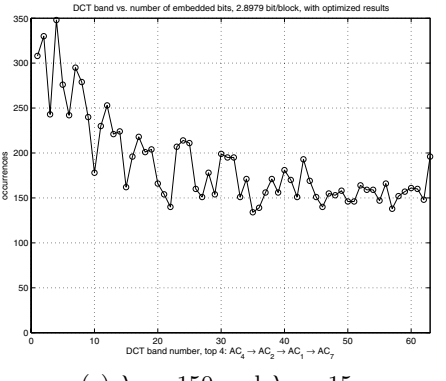

(c) $\lambda_1 = 150$ and $\lambda_2 = 15$

Fig. 1.8. Comparisons of the histograms of embedding coefficients with different weighting factors in Eq. (1.3)

JPEG attack, BCR = 0.9013 | LPF attack, BCR = 0.7199 | MF attack, BCR = 0.8103

(a) Results with $\lambda_1 = 50$ and $\lambda_2 = 15$

JPEG attack, BCR = 0.9402 | LPF attack, BCR = 0.8268 | MF attack, BCR = 0.8959

(b) Results with $\lambda_1 = 100$ and $\lambda_2 = 15$

JPEG attack, BCR = 0.9530 | LPF attack, BCR = 0.8268 | MF attack, BCR = 0.8959

(c) Results with $\lambda_1 = 150$ and $\lambda_2 = 15$

Fig. 1.9. Comparisons of the extracted watermarks and BCR values with different weighting factors in Eq. (1.3)

Furthermore, we can easily see that the BCR values after LPF attack are much lower than their counterparts after MF and JPEG attacks. To alleviate this problem, the weighting factor associated with robustness, λ_1, should be increased to enhance the contribution from the robustness in the fitness function. Comparing the three sets of data with $(\lambda_1, \lambda_2) = (50, 15)$, $(100, 15)$, and $(150, 15)$ for instance, we observe that by simply increasing the value of λ_1, both the resulting PSNR and capacity get decreased. Figure 1.9 also demonstrate this observation from subjective point of view.

Summing up, the weighting factors need to be carefully chosen based on twofold. The first is that contributions from the different requirements are supposed to have nearly equal contribution. The second is that both the watermarked image and extracted watermark need to be recognized from subjective point of view.

Table 1.3. Comparisons of imperceptibility (in dB), robustness, and capacity (in bit/block) with different a combination of attacks. Weighting factors are set to be $(\lambda_1, \lambda_2) = (50, 10)$. To simplify the representation, we use the abbreviations of J, L, and M to represent JPEG, LPF, and MF, respectively.

Attack	PSNR (dB)	BCR (JPG)	BCR (LPF)	BCR (MF)	Capacity (bit/block)	The two best bands
J	45.91	0.9603	*0.7128*	*0.7469*	3.4285	$AC_{16} \rightarrow AC_{14}$
L	46.44	*0.9194*	0.8380	*0.7963*	3.2273	$AC_1 \rightarrow AC_4$
M	43.45	*0.9058*	*0.7947*	0.8486	3.3423	$AC_1 \rightarrow AC_4$
J & L	46.45	0.9262	0.8395	*0.7955*	3.1863	$AC_4 \rightarrow AC_1$
J & M	43.56	0.9107	*0.7500*	0.8718	3.3145	$AC_1 \rightarrow AC_4$
L & M	46.21	*0.9058*	0.7947	0.8486	3.3081	$AC_4 \rightarrow AC_2$
J & L & M	45.46	0.9196	0.7897	0.8484	3.3364	$AC_4 \rightarrow AC_2$

1.5.2 Combination of Various Attacks

Based on the building blocks in Figure 1.1, algorithm designer can choose different attacks for making optimization. We show the combination of various attacks with GA in Table 1.3 as follows.

In Table 1.3, we list all the seven combinations from the three independent attacks with the weighting factors of $\lambda_1 = 50$ and $\lambda_2 = 10$. The BCR values, shown in italics, are not optimized based on the type of attacks. For instance, for the results with JPEG-type attack in the first row, numerical values for $BCR_{(LPF)}$ and $BCR_{(MF)}$ are shown in italics, because only $BCR_{(JPG)}$ is optimized. Because we embed the watermark into DCT coefficients, it seems that our algorithm tends to resist JPEG attack inherently. Therefore, in the first three rows, we can see that BCR values after JPEG attacks are high enough, and we need to take the LPF or MF attack into optimization to obtain the improved BCR values. In the fourth to sixth rows, we can see that only the BCR values with selected attacks perform better. In the last row, because we calculate the average BCR value in the fitness function in Eq. (1.3), if we choose all the three attacks altogether, $BCR_{(JPG)}$ tends to perform better inherently. Therefore, the two remaining BCR values may get decreased, and we can see that the numerical results present this phenomenon.

Summing up, our algorithm tends to resist JPEG attack based on its characteristics. And we may suggest to ignore the JPEG attack during the optimization process. By choosing the combination of LPF and MF attacks into the fitness function, acceptable results can be reached.

1.6 Conclusions

In this chapter, we discussed about the optimization of robust watermarking with genetic algorithms. By finding trade-offs among robustness, capacity, and imperceptibility, we design a practical fitness function for optimization.

We observe that the three requirements conflict with one another, thus, by applying GA, we can obtain the optimized outcome. Simulation results depict the improvements of our algorithm, hence the implementation of copyright protection system, and it is directly extendable to cope with a variety of attacks in the benchmarks. Since the capacity can be set variable here, corresponding results perform better than those in literature [12] with fixed watermarking capacity. In addition, the weighting factors in the fitness function play an important role in the design of algorithm. Properly selected weighting factors can lead to better results in overall performance. Other schemes, such as employing ECC into the watermark, can be considered to be integrated into our implementation to obtain better performance with a slight increase in watermark encoding and decoding.

References

1. Gen, M., Cheng, R.: Genetic Algorithms and Engineering Design. Wiley, New York (1997)
2. Huang, H.C., Pan, J.S., Huang, Y.H., Wang, F.H., Huang, K.C.: Progressive watermarking techniques using genetic algorithms. Circuits, Systems, and Signal Processing 26, 671–687 (2007)
3. Koenen, R.H., Lacy, J., Mackay, M., Mitchell, S.: The long march to interoperable digital rights management. Proc. of the IEEE 92, 883–897 (2004)
4. Macq, B., Dittmann, J., Delp, E.J.: Benchmarking of image watermarking algorithms for digital rights management. Proc. of the IEEE 92, 971–984 (2004)
5. Morelos-Zaragoza, R.H.: The Art of Error Correcting Coding, 2nd edn. Wiley, New York (2006)
6. Pan, J.S., Huang, H.C., Jain, L.C. (eds.): Intelligent Watermarking Techniques, pp. 3–38. World Scientific Publishing Company, Singapore (2004)
7. Pan, J.S., Huang, H.C., Jain, L.C., Fang, W.C. (eds.): Intelligent Multimedia Data Hiding. Springer, Heidelberg (2007)
8. Petitcolas, F.A.P.: Stirmark benchmark 4.0 (2004), `http://www.petitcolas.net/fabien/watermarking/stirmark/`
9. Piva, A., Bartolini, F., Barni, M.: Managing copyright in open networks. IEEE Internet Comput. 6, 18–26 (2002)
10. Shehab, M., Bertino, E., Ghafoor, A.: Watermarking relational databases using optimization-based techniques. IEEE Trans. on Knowledge and Data Engineering 20, 116–129 (2008)
11. Shieh, C.S., Huang, H.C., Wang, F.H., Pan, J.S.: An embedding algorithm for multiple watermarks. Journal of Information Science and Engineering 19, 381–395 (2003)
12. Shieh, C.S., Huang, H.C., Wang, F.H., Pan, J.S.: Genetic watermarking based on transform domain techniques. Patt. Recog. 37, 555–565 (2004)
13. Wang, S., Zheng, D., Zhao, J., Tam, W.J., Speranza, F.: An image quality evaluation method based on digital watermarking. IEEE Trans. Circuits and Systems for Video Technology 17, 98–105 (2007)